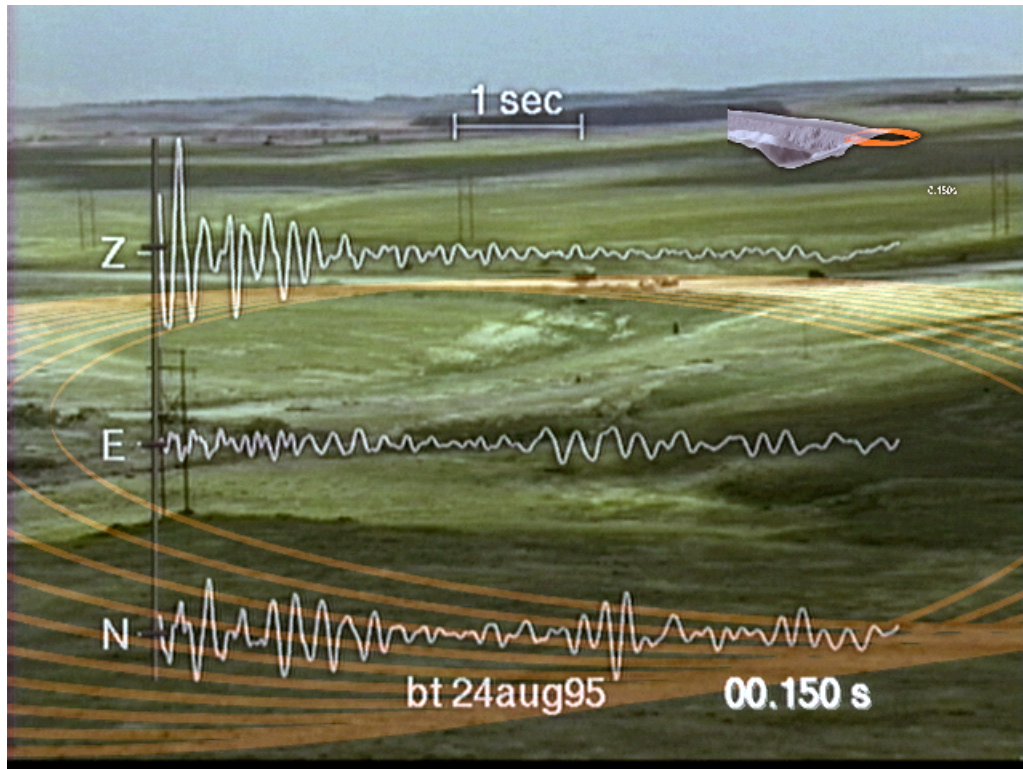


# ANALYSIS OF MINING EXPLOSION PERFORMANCE WITH MULTIPLE SENSOR DATA AND PHYSICAL MODELS



Brian W. Stump and David P. Anderson  
Department of Geological Sciences, Southern Methodist University  
Dallas, Texas

D. Craig Pearson  
Geophysics Group, Los Alamos National Laboratory  
Los Alamos, New Mexico

Robert Martin  
Thunder Basin Coal Company  
Wright, Wyoming

## **1. Introduction and Motivation**

## **2. Tools for Multidimensional Documentation**

- Data Recording
  - *Image Data*
  - *Ground Motion and Acoustic Data*
  - *Digitizing Video*
  - *Standard Video Data*
  - *Digital Bandwidth*
  - *Digitizing and Data Archival Method*
- Video Data Processing
  - *De-interlace*
  - *Camera Motion Correction*
  - *Interpolation*
  - *Time stamp*
- Combining Video and Waveform Data
  - *Waveforms*
  - *Moving Cursor*
- Incorporation of Models in Visualization
  - *Two-Dimensional Blast Model*
  - *Three-Dimensional Blast Models*

## **3. Applications to Different Types of Mining Explosions**

- Single Shot
- Cast Blast
- Coal Fragmentation

- Hard Rock Fragmentation
- Soft Rock Bulking

#### **4. Results**

- Overcoming Frame Rate Limitations of Video Data
- Effect of Blast Design on Near-Source Seismograms
- Different Types of Cast Blasts
- Multiple Angle Images of Blast
- Documentation of Damage

#### **5. Conclusions**

#### **6. Future Development of New Tools**

#### **7. References**

#### **8. Acknowledgments**

## **1. Introduction and Motivation**

Mining explosions designed to move, bulk or fracture rock are often composed of a number of explosions arranged in a complex spatial and temporal pattern. The effects of the explosions are strongly dependent upon the design and implementation of this blasting pattern. This paper describes the collection, combination and visual display of multiple types of data from these explosions for the purposes of understanding the relationships between the blast design, implementation, and observations.

Data sets can consist of three-component ground motion, acoustic, video and high speed film, three-dimensional topography, geological and geophysical properties, design blast pattern and timing, and velocity of detonation in the explosive for individual borehole detonation times. The explosions studied include simple single-fired contained explosions, ones designed to bulk and fracture rocks and those that cast material.

Direct comparison of the data with blast models in a visual format provides the mechanism to identify subtle differences between the two that may lead to new insights into the blasting practice. The tools developed for these comparisons are designed to capture the three-dimensional spatial aspects of the problems as well as the time varying characteristics. Single and multiple data frames from the analysis of the different explosions are included in this paper. Time varying images or movies are available for the explosions analyzed in this study on an accompanying compact disk (CD). These data displays provide the reader the capability to move forward and backwards through the data set at any speed, isolating processes of interest.

Despite the fact that this study is only exploratory in nature and limited in scope, the visualization tools have been used to identify: (1) Out of sequence detonations; (2) Simultaneous detonation of multiple boreholes; (3) Time sequencing leading to confinement problems; (4) Coal damage from cast blasting; (5) Timing of cast impact; (6) Free-face stress wave interaction times; and (7) Compressional seismic energy superposition. The combination of the multiple data sets provides the linkage between these physical phenomena and their resulting effects, such as material movement, fragmentation, ground motions and acoustic energy.

The final step in this analysis is the introduction of modified blasting practices that can provide improved blasting results in the mine. The key to this last step is the transfer of the tools discussed in this paper to the engineer in the mine so that they can be applied as part of a normal blasting program. The instrumentation techniques and analysis tools were developed with these goals in mind.

The paper has three sections. The first discusses the tools for analyzing video, ground motion and acoustic data. The combination of models of the blast with these data sets is illustrated. The second section illustrates the visualization tools with application to five different types of mining explosions. The third section discusses new insights and results provided by this analysis.



## **2. Tools for Multidimensional Documentation and Visualization**

The goal of this work is the documentation of physical phenomena that are important in near-surface blasting. The observational tools introduced are intended to quantify processes that effect mine productivity, safety, ground motion and air blast. Multiple data sets such as three-dimensional topography, geological and geophysical structure, design blasting pattern, ground motions, acoustic data, video/high speed film and material characterization data provide the constraints for quantifying the blasts. Physical and mathematical models of the blasting process are used in the interpretation of the data. Comparison of the data with the models identifies constraints on the models as well as suggesting improvements to blasting practices.

The multidimensional nature of typical mining explosions has led to the new approaches to combining data and models. Key to the comparison and combination of disparate data sets is access to digital data. Ground motion and acoustic data are typically collected in this format. Equipment for acquiring or converting video and high-speed film to digital format are available. The synthetic models are computationally derived and so are also digital. GPS (Global Positioning System) time and location tags provide the basis for absolute correlation of the different data sets, even when they are recorded at different spatial locations. Not all the data in this report are currently recorded in digital form nor does it all have GPS time and location tags. Approaches for data correlation using incomplete data sets are discussed and demonstrated.

Visual tools are found to be effective when a number of different types of data must be interpreted simultaneously. The time varying characteristics of the problem are investigated by combining a number of images into a movie format (see accompanying CD). Interaction with models and data in this time varying format provides a mechanism for quantification of similarities and differences in the two, leading to improved understanding of the blasting process.

- **Data Recording**

Documentation of the explosions begins with the acquisition of the different types of observational data. The characteristics of the video and ground motion/acoustic data acquisition are described.

- **Image Data**

Blasts were recorded on Hi-8 video cameras at 30 frames per second with shutter speeds as high as 1/10000 second (Stump *et al.*, 1996; Pood and Gilbert, 1996). These cameras were chosen over standard VHS and 8mm because of their improved resolution while retaining relatively low cost. In order to produce multiple perspective images of a blasts that can later be correlated, cameras for some experiments had Genlock capability (locking to an externally generated synchronization signal such that the scans of the two cameras represent identical temporal events).

High-speed film with frame rates between 500 and 1000 have been used to document millisecond delay blasting. Systems utilizing high-speed video data acquisition have been recently described (Chung, 1996). Pood and Gilbert (1996)

discuss the advantages of high frame rate documentation of mining explosions. They note that the 30 frames/s sample rate of typical video acquisition is unable to resolve many blasting effects. De-interlacing of standard video (discussed in a subsequent section) provides sampling of 60 fields/s, which these authors find adequate for many mining applications. An interpolation scheme utilized between fields can produce 120 images/s or a time interval between images of 8.33 ms. The order of magnitude cost difference between standard video acquisition (60 fields/s) and high-speed video (up to and beyond 1500 frames/sec) precludes the routine application of high-speed video in standard mining operations.

In addition to cost limitations, high-speed video involves large data rates and associated computer memory and storage requirements. A standard 640 by 486 pixel video image is approximately one megabyte of information (see Digital Bandwidth), resulting in data rates approaching a gigabyte per second for full-resolution high-speed digital video. These data rates require some type of data compression either in the spatial resolution (reduction in the number of pixels in a frame), the dynamic range (the number of bits used to represent each pixel) or the sampling time. Utilization of standard Hi-8 video provides a low cost alternative at the expense of reduced sampling rate in time (60 fields/sec) while retaining full spatial resolution (640 x 486 pixels) and high dynamic range (24 bit per pixel). The order of magnitude cost reduction and the ease of near real-time viewing of images makes this a useful alternative.

Standard video cameras can be deployed up to 30 minutes before a shot and left unattended for over an hour. This characteristic is not available with high-speed film or video and thus provides the opportunity for improved spatial resolution (multiple unattended cameras) of explosions as well as the characterization of the blast in regions typically inaccessible to the blaster during the explosion. Information from regions such as the pit during a cast blast is shown to be critical to the understanding of effects from some explosions.

An example of a camera deployment in a mining operation is given in Figure 1.



Figure 1. Installation of a Sony EVW-300 Hi-8 video camera overlooking a cast shot. The coax cable is connected to a companion camera so that they are Genlocked (frame-by-frame sync between two cameras).

Cameras are placed as close as 100 m from a single cylindrical charge, parallel with the free face in front of the charge. Larger, millisecond delay-fired explosions

necessitate separation between the explosions and the camera as great as a kilometer. It has been found useful to deploy cameras both in front (above the free surface if possible) and in back of the bench on which multiple-hole explosions are detonated, as well as in the pit where material will be cast. Multiple cameras are useful in the characterization of explosions of large spatial dimension such as those accompanying surface coal casting operations. The different views of the blast provide the data to quantify the performance of the individual explosions in the array as well as constrain the timing of secondary source phenomena such as material cast into the pit.

#### ▪ Ground Motion and Acoustic Data

Velocity and acceleration waveforms were acquired with a 16-bit Refraction Technology Data Acquisition System, Terra Technology accelerometers and Sprengnether S-6000 2 Hz seismometers. The seismometers are used in the quantification of the near-regional (several to tens of kilometers) wave field while the accelerometers are deployed very close to the blasts (tens to hundreds of meters, near-source) providing good azimuthal as well as range coverage of the test bed. The data are sampled at 250 or 500 samples/s in order to characterize the waveforms in as broad a frequency band as possible. An example instrument deployment is given in Figures 2 and 3.

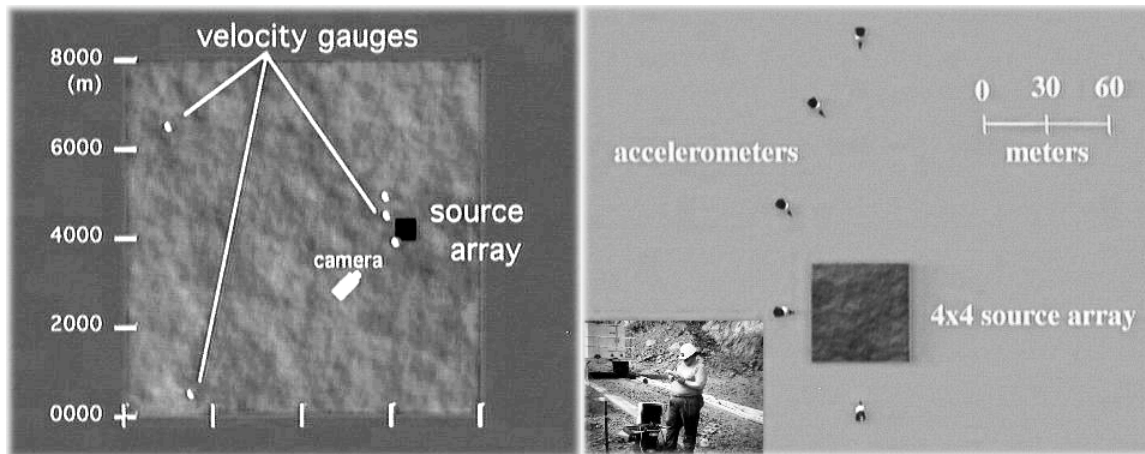


Figure 2 (left). Near-regional instrumentation plan illustrating the utilization of velocity transducers and cameras to document explosion processes. Figure 3 (right). Near-source instrumentation plan illustrating the installation of one of the accelerometers and accompanying data acquisition units. The source in this case is a 4x4 array of cylindrical boreholes detonated sequentially.

Consideration needs to be given to the separation distance of the ground motion instrument and the explosions relative to the total dimension of the explosive array. If the distance from the gauge to the nearest explosive borehole is comparable or less than the total spatial dimension of the explosive array, then the differences in spatial distance from each individual explosion to the receiver will dominate the observations (Reamer *et al.*, 1994). If the purpose of the ground motion measurement is to quantify the relative performance of each individual borehole, it is best to deploy seismic instruments several source dimensions from the explosive array. Propagation path distances from each borehole to the receiver are approximately equal in this configuration providing data to quantify differences between boreholes.

- **Digitizing Video**

Key to the combination and analysis of different data sets is access to all the data in digital form. A number of techniques and types of equipment are available to generate digital video. We will focus on digitizing standard video data since these types of cameras are already a part of many mine documentation programs.

- **Standard Video Data**

The two most common video formats are NTSC and PAL (work discussed in this paper has focused on NTSC format data). These video standards were designed to produce visual images by repetitively sweeping an electron beam over a cathode-ray tube. This beam moves horizontally from top to bottom in a fixed number of lines, which are modulated in intensity, freeing electrons and emitting photons from the phosphor-coated front surface. The vertical resolution of the image is set by the number of scan lines (about 500) and the horizontal resolution is determined by frequency response of the modulation circuitry and the bandwidth of the driving signal (about 700).

NTSC video frame rate is defined as 30 frames per second (fps) (although for historical reasons it is 29.97 fps) but the video image is actually updated to the screen at 60 Hz to reduce image flicker through a process called "interlacing." Interlaced frames contain two distinct image "fields" which consist of all even and all odd numbered scan lines. The video hardware draws half of the image (every other line) and then the other half 30 times per second (Figure 4).

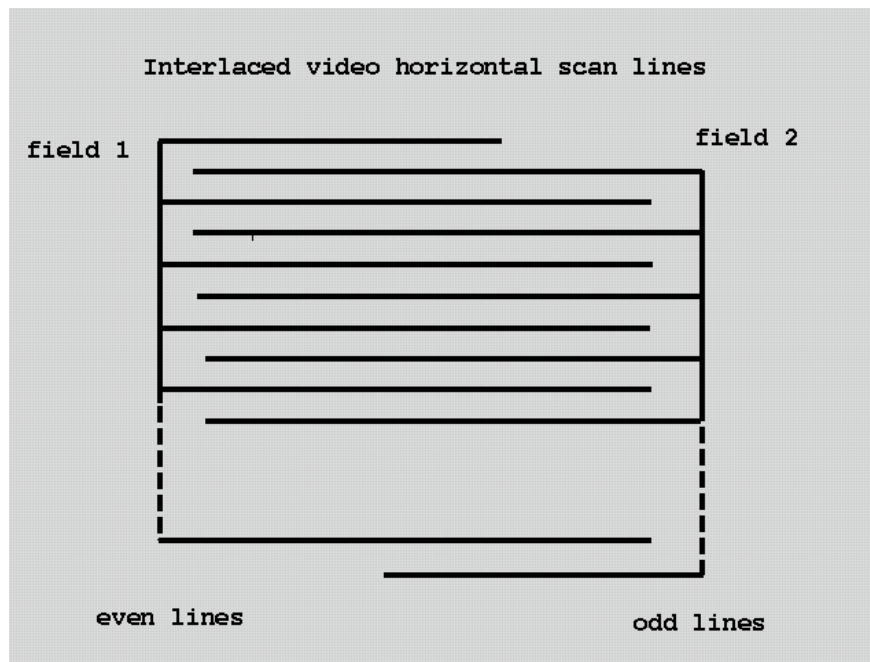


Figure 4. A single video frame is composed of two fields, one for all even numbered scan lines and one for all odd numbered scan lines. The video frame rate is 30 frames/s while the field rate is 60 fields/s.

The two fields that make up a frame produce a single new image every 33 ms (30 Hz). The individual fields are separated by 16.66 ms (60 Hz). This time difference



can be exploited digitally to increase the video temporal resolution. A single video frame from a coal shot is reproduced in Figure 5. The blurring in the image is a result of interlacing of two fields separated by 16.67 ms.

#### ▪ **Digital Bandwidth**

NTSC video produced by Hi-8 cameras can be digitized into discrete pixel images through video-digitizers or "frame-grabbers" available on a number of different computing platforms. One practical characteristic of such systems is the digital bandwidth and throughput of the computer and disk drives. A common digital representation of an NTSC video frame (both fields) is a 640-by 486 pixel image with three-color bit-planes of 8 bits each (24 bit color, also called RGB, or component color).

$$640 \times 486 \times 3 = 933120 \text{ bytes per frame.}$$

A useful approximation is 1 megabyte per frame. At 30 fps that is 30 megabytes per second, or 1.8 gigabytes per minute. These are high-sustained data rates by contemporary computing standards, and most hardware cannot maintain the necessary throughput for video playback and recording. Common implementations use either special hardware compression/decompression techniques to reduce the required bandwidth, or reduce the resolution of the video input by down sampling or using low-resolution monochrome cameras.

A new generation of lower cost consumer digital video cameras are now available and preclude the need for digitization but require an equivalent set of hardware for decoding the compressed video images stored on tape by these cameras. Typically some type of image compression is applied prior to storage in digital format on tape in these cameras as well.

#### ▪ **Digitizing and Data Archival Method**

A hybrid process is currently used to digitize and store Hi-8 video using a Sony CVR 5000 laser disk and a Silicon Graphics Indigo2 Workstation with a Galileo video card. The Hi-8 tape is played back and recorded on the Sony CVR 5000 laser disk using the SGI Indigo2 as a "time-base corrector" to compensate for data rate errors inherent in the analog video media and to assure that no frames are duplicated or dropped.

The laser disk is a write-once media that stores 43,500 video frames on each side of a removable media disk, making it cost effective for high resolution component video data archival (~\$400 per disk). Once the data is stored on laser disk, it is digitized frame-by-frame from the laser disk and transferred to hard disk using the SGI Galileo video card. This process produces digital RGB format color images each 640x486 pixels with each pixel representing 24 bits of color information. A digitized frame from a coal shot is shown in Figure 5.

With typical blasts lasting between 5 and 20 seconds, a single video data volume of an explosion is between 150 and 600 Mbytes. It is important to have large disks and computer memory for effective processing of these data sets. Compression algorithms such as JPEG or MPEG can be used to reduce the size of these files with some loss of resolution, although fast hardware implementations of these compression schemes are best for rapid data review.

- **Video Data Processing**

The image data recovered from the video cameras provides the foundation for the quantification of the mining explosions. The other data sets are compared to it for purposes of interpretation. Four processing steps are applied to the digitized video images before they are combined with the seismic and acoustic waveform data. The images are de-interlaced, effects of camera motion are removed (if required), intermediate frames are interpolated, and the resulting frame is given a unique time-stamp.

- **De-interlace**

Each digital video frame is separated into even and odd fields. This produces half frames that are 640x243 pixels with every other scan line missing.



Figure 5: Interlaced video frame from a coal explosion. The frame is 640 by 486 pixels and is made up of two fields each 16.67 ms apart in time.

The missing scan lines are generated by linearly interpolating the pixels on the adjacent lines, and a full frame 640x486 is constructed from each half-frame. This removes the blur associated with the movement of material from one field to the next, and permits field-by-field viewing of the blast. The process produces 60 unique video representations of the explosion every second for a sampling interval of 16.67 ms. A de-interlaced image from the video data in Figure 5 is reproduced in Figure 6. The fuzziness is eliminated.

- **Camera Motion Correction**

Cameras at blast sites may vibrate as the tripod responds to seismic and acoustic energy. This motion can be minimized by tightly coupling the tripod to the ground (apply sandbags and bury the legs) but some residual motion may remain. This motion manifests itself as a periodic oscillation of the image. The technique used to remove camera motion is to note the location of a fixed point or points in the image and to translate the image such that these points remain stationary. This correction is accomplished with standard image processing tools for image rotation, translation, and cropping. Many of the consumer grade video cameras offer image stabilization during recording that can preclude the need for these corrections.



Figure 6: One of the fields from the frame displayed in Figure 5. The image has been interpolated and time tagged. Elapsed time since the first motion in the video is given in the lower right hand corner.

- **Interpolation**

The images are passed through a temporal interpolation filter, which generates a synthetic image for each pair of input images. This process smoothes the transitions between frames created from all even or all odd scan lines, and gives a final data rate of 120 images/s, with a resolution of 8.33 ms per image.

- **Time stamp**

Time stamps are important when studying the video image-by-image. Each final image is given an individual time stamp by the SGI rendering hardware. These are



typically applied to one corner and record accumulated time from the start of the shot. The start time can be taken from the end of the countdown on the audio channel, the flash of the ignition system in the video, or the first movement of material.

Some video cameras have the ability to record a GPS (Global Positioning System) data stream along with video and audio, which includes time as well as location information. This allows the video to be synchronized precisely with seismic signals, which are also locked to GPS.

- **Combining Video and Waveform Data**

The video images capture near-surface phenomena during the blast such as the detonation sequence, degree of explosive confinement for individual boreholes, the amount and timing of material cast and possibly some wave propagation phenomena such as the interaction of the stress wave with the free surface or free face. Energy coupled into the ground and air also quantifies the blasting process and provides supplemental diagnostics. Combining the video, ground motion and acoustic data into a single image provides enhanced documentation of the blasting processes. The approach to this combination process is next described.

- **Waveforms**

A common method for displaying seismic and acoustic data is as waveform plots in two-dimensional Cartesian space. The vertical or 'y' axis represents the ground velocity or acceleration at each time point while the horizontal or 'x' axis represents time increasing to the right. Various common software utilities such as spread sheets, databases, and higher math tools include the ability to create these 2D and even 3D waveform representations of arbitrary data sets. These can then be combined with time-aligned digital video images through a process called "compositing."

A slightly more complex method for creating the waveform images makes use of generic rendering software and hardware available on the Silicon Graphics Indigo2 Workstation and other computers. The raw seismic data is filtered through the data processing software developed in the Geophysical Imaging Laboratory at SMU, the output of which directly drives an OpenGL graphics engine. This second approach allows high quality, anti-aliased waveforms to be rendered, which can be seamlessly integrated with the video frames. It also provides the ability to generate other 3D geometric shapes as part of the same image. This method is used to create a moving cursor bar, blast timing model, and particle motion displays discussed later.

Figure 7 illustrates a de-interlaced and processed video field with composited waveforms. The three waveforms are ground velocities (Z-vertical, E-east/west, N-north/south) recorded approximately 10 km from the explosion.

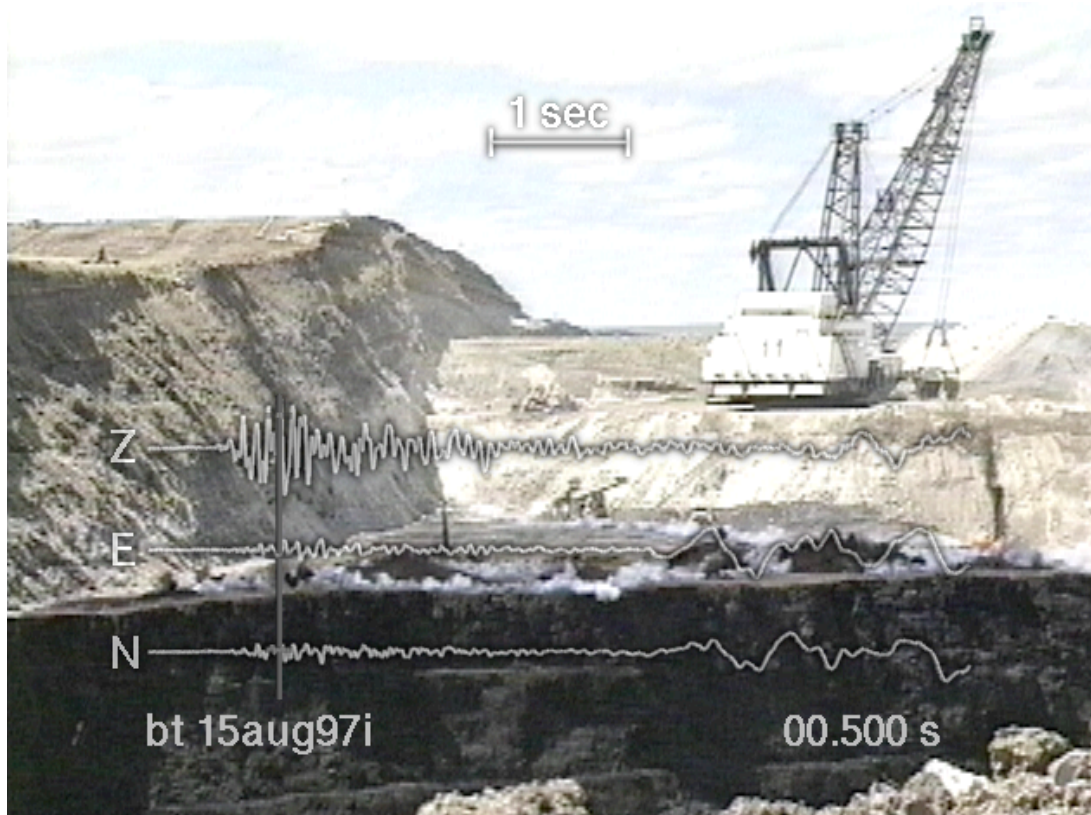


Figure 7: De-interlaced video images with waveforms mapped onto the image. The vertical bar across the three waveforms represents the time in the video image.

#### ▪ *Moving Cursor*

The combination of blast video and seismic/acoustic waveforms requires some method of temporal coordination linking the data sets. The moving cursor bar is used for this task. It marks the point on the waveform or waveforms that correspond to the current video image. The cursor and the waveforms are rendered by the graphics engine as 3D objects with a unique location for each frame. Figure 7 illustrates a moving vertical cursor bar at one time interval, 0.5s.

There are several possible approaches to aligning the seismic and video data. The finite speed of seismic waves constrains the seismic data to be collected later in time than the video of the event which produced the wave; light travels faster than sound. The same is true of the acoustic channel. Accurate alignment of the seismic and video data would show the seismic signals arriving after their visual counterparts and the acoustic signals thereafter. A more intuitive arrangement which provides increased physical insight into the blasting process is to subtract the seismic travel times from the data and align the waveforms with the source event on the video. The acoustic channel can be handled similarly. Experience has shown that engineers and seismologists analyzing shot performance prefer this alignment.

The mining explosions displayed in this paper will be characterized by reproducing four images separated in time. The location of the cursor bar and the time stamp in the image provide the necessary information for correlating the multiple images.

- **Incorporation of Models in Visualization**

The last step in the data processing and interpretation is the inclusion of models of the blast for comparison to the data. The model can be quite simple such as two-dimensional map of the blast or more complex including the detonation times of each individual explosion in three-dimensions.

Comparison of blast models to the data is an iterative process. The approach to modeling in this paper is to begin with a simple characterization of the mining explosion and its resulting phenomena. Combining models and data can be used to identify differences that can be as simple as departures of design and actual detonation times. Models can be sampled at a finer temporal scale than the data. When comparing to video data, models provide a tool for interpolation between data points and identification of phenomena that might be aliased by the data-sampling rate.

- ***Two-Dimensional Blast Model***

The simplest model of the explosion captures the two-dimensional distribution of boreholes in plan view.



Figure 8: Same as Figure 7 with a simple two-dimensional model of the blast time correlated with video and ground motions. Pixels in the model represent individual blast holes and turn from white to red at design detonation time.



The model has a small transparent colored square for each borehole in the pattern that changes color at detonation time. Delay-fired shots can be seen to move across the model. When combined with video of the blast, similarities and differences between designed and actual blast performance may be observed. Figure 8 takes the same blast used previously and includes a simple two-dimensional model in the lower center of the image. The blast in this image is about 60% complete as denoted by the large number of boreholes that have turned red in the model. The effects of the already detonated holes can be seen in the video as well as the ground motion record. Several of the boreholes have vented to the atmosphere. It is difficult to determine which boreholes have vented by comparing the two-dimensional shot model with the video since the perspectives are different.

### ▪ *Three-Dimensional Blast Models*

Our ultimate goal is the direct mapping of the models of the blast onto the video images. The identification of processes in different spatial and temporal locations (such as the venting noted in Figure 8) in a single blast can then be more easily localized. A three-dimensional model can be used to directly overlay the video. A frame that incorporates a three-dimensional shot model is given in Figure 9. The model also includes a characterization of the generation and propagation of compressional energy from each borehole. At the design detonation time for each borehole, a small sphere appears and generates a cylindrical ring that expands in radius at the compressional velocity for the material around the explosion.

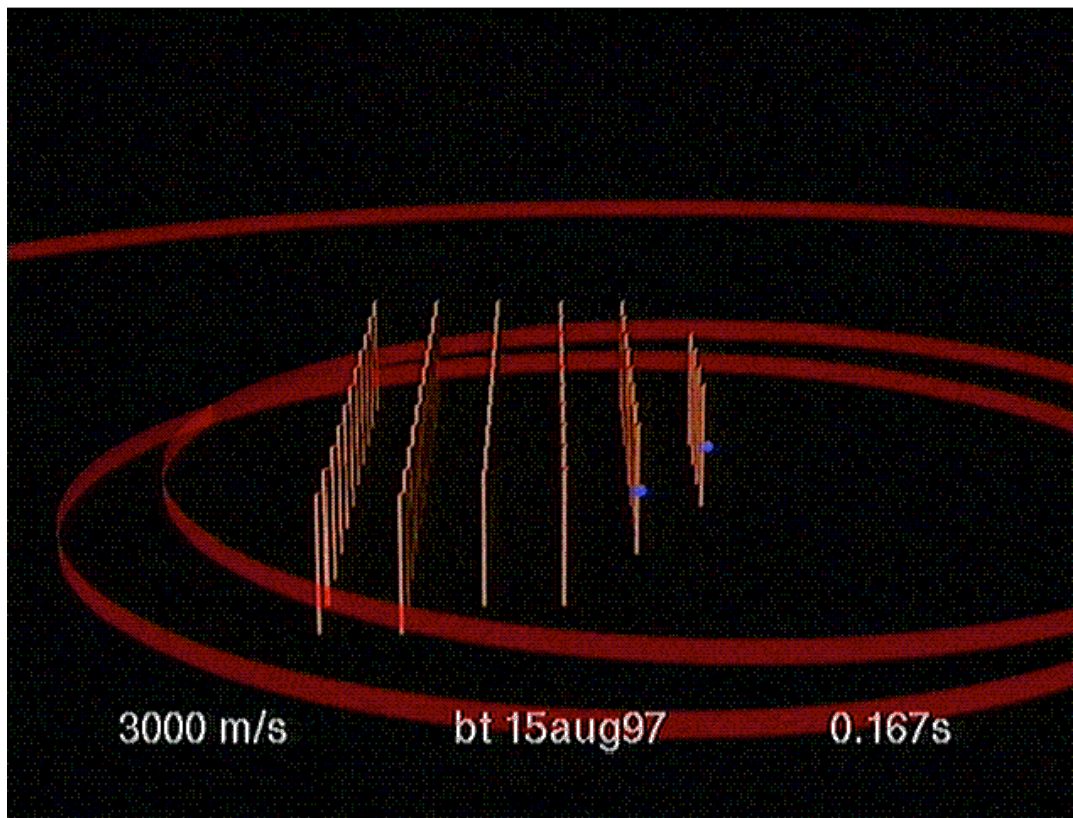


Figure 9: Three-dimensional model of the blast. The boreholes are represented by the rows of cylinders. At the design detonation time a ball appears at the center of the appropriate borehole and generates a red ring that expands in radius at the compressional velocity of the material.

The three-dimensional blast model is superimposed on the video data in Figure 10. Several of the boreholes have already detonated and the resulting spreading compressional energy is included. Despite the fact that a number of boreholes have detonated in the front row, one can see that there are many boreholes on the left-hand side of the shot that remain undetonated. As with all the images in this report, there are accompanying movies that combine all the data images in sequence.

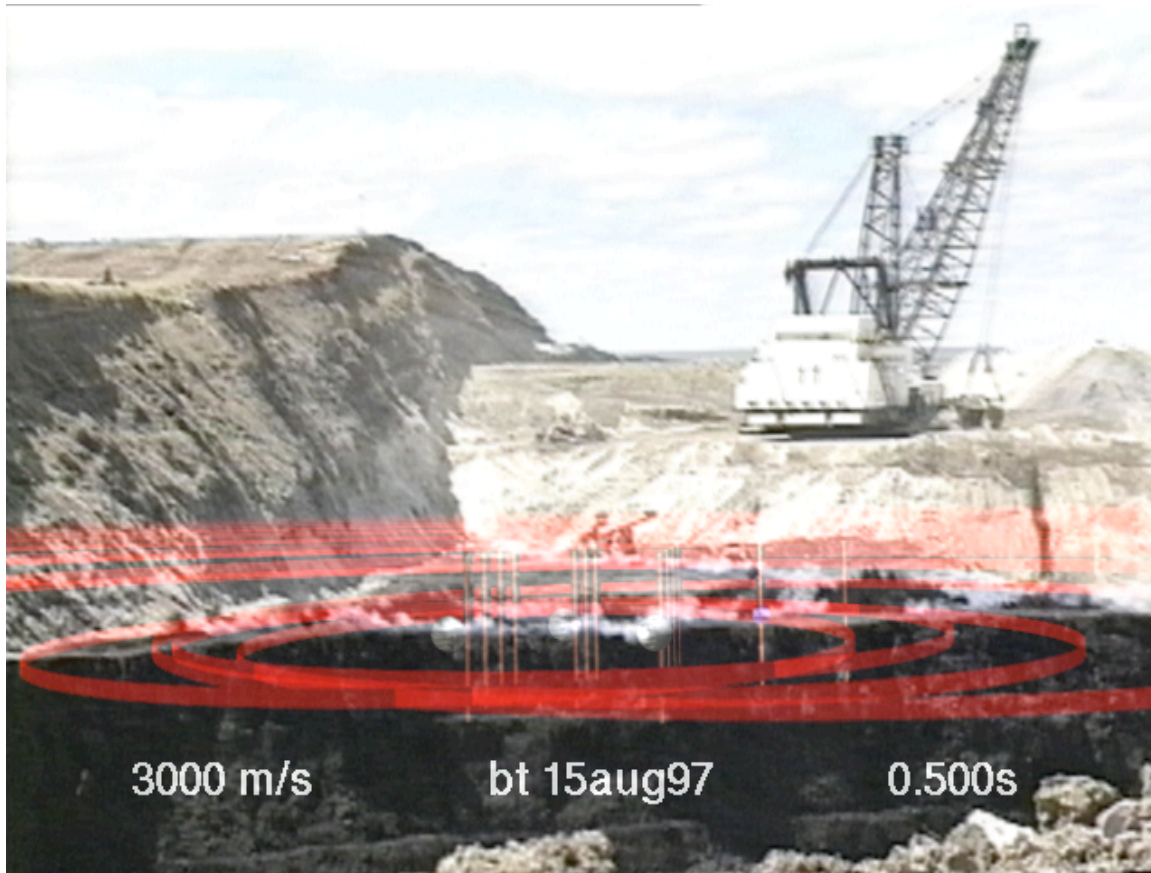


Figure 10: The same image and model as that reproduced in Figures 7 and 8 but now a three-dimensional model of the blast like that in Figure 9 is mapped onto the appropriate video image of the actual explosion.

### **3. Applications to Different Types of Mining Explosions**

The data and model visualization tools introduced in the previous section are applied to five different blasts: (1) Single shot; (2) Cast Blast; (3) Coal Fragmentation; (4) Hard Rock Fragmentation; and (5) Soft Rock Bulking. These shots span a range of blasting environments allowing the effects of shot timing, compressional wave generation and interaction, fragmentation and casting to be illustrated.

- **Single Shot**

The single shot is a simultaneously detonated, multiple borehole, and contained explosion. Ten vertical boreholes were drilled to depths ranging from 118 to 139 feet at 34 foot spacing along a north-south trending line. They were loaded with an average of 5,000 pounds of explosives and stemmed with 40 to 61 feet of material. All holes were detonated simultaneously.

De-interlaced video images combined with ground velocity records from the explosion are reproduced in Figure 11a. The three-component velocity instrument was located approximately 12 km north-northwest of the shot. These more distant seismic records are used for interpretation purposes to assure that the propagation path differences between the individual boreholes is minimized allowing the relative comparison of the individual coupling from each of the boreholes.

Four images of the blast are included in Figure 11a providing the basis for assessing explosion phenomena and the resulting waveforms. A 60 field/s movie of this explosion (and all other explosions) is available for more detailed analysis on the accompanying CD. The short duration (less than 0.5 s) of the dominantly vertical ground velocity is a result of the simultaneous detonation of the explosions. Since the seismic station is nearly north of the shot, the north-south motion (N in figure) is primarily radial while the east-west motion (E in figure) is primarily transverse. The explosion generates little transverse motion and only slightly more radial. The dominance of the vertical motion is consistent with the compressional source, particularly where the instrument is emplaced in a low velocity surficial layer and the compressive energy is refracted to the vertical at the receiver.

The video images document the containment of the explosives with 40 to 61 feet of stemming for the first 1.650 s. Images at latter time reveal a release of explosive byproducts to the atmosphere several seconds after the detonation. This long-time containment failure is assumed to have little affect on the radiated seismic energy as its characteristic time function is well outside the bandwidth of the seismic data.

Careful inspection of the video images reveals evidence of secondary source phenomena. The explosion was conducted in the late summer when near surface moisture content was low. The interaction of the compressive wave from the contained explosion with the free surface can fail the surface layers in tension, lofting these materials, a process known as spallation. When these failed materials re-impact as a result of gravity, areas that are barren of natural grasses and plants produce dust. The spall closure signature (dust cloud) is apparent in the images at 0.517 s and 1.650 s. The light colored areas at 0.517 s that are in the center of the images, vertically, and to the far left and right, horizontally, show this effect as an increased reflectance. The area of increased reflectance moves to the center of the image at 1.650 s as spall closure propagates back to directly above the explosion (ground zero). The video images capture the timing of the spall process.



Comparison of this timing with the observed velocity records suggests that within the bandwidth of the velocity instrument (1 Hz) that spall closure is secondary to the generation of the seismic energy.

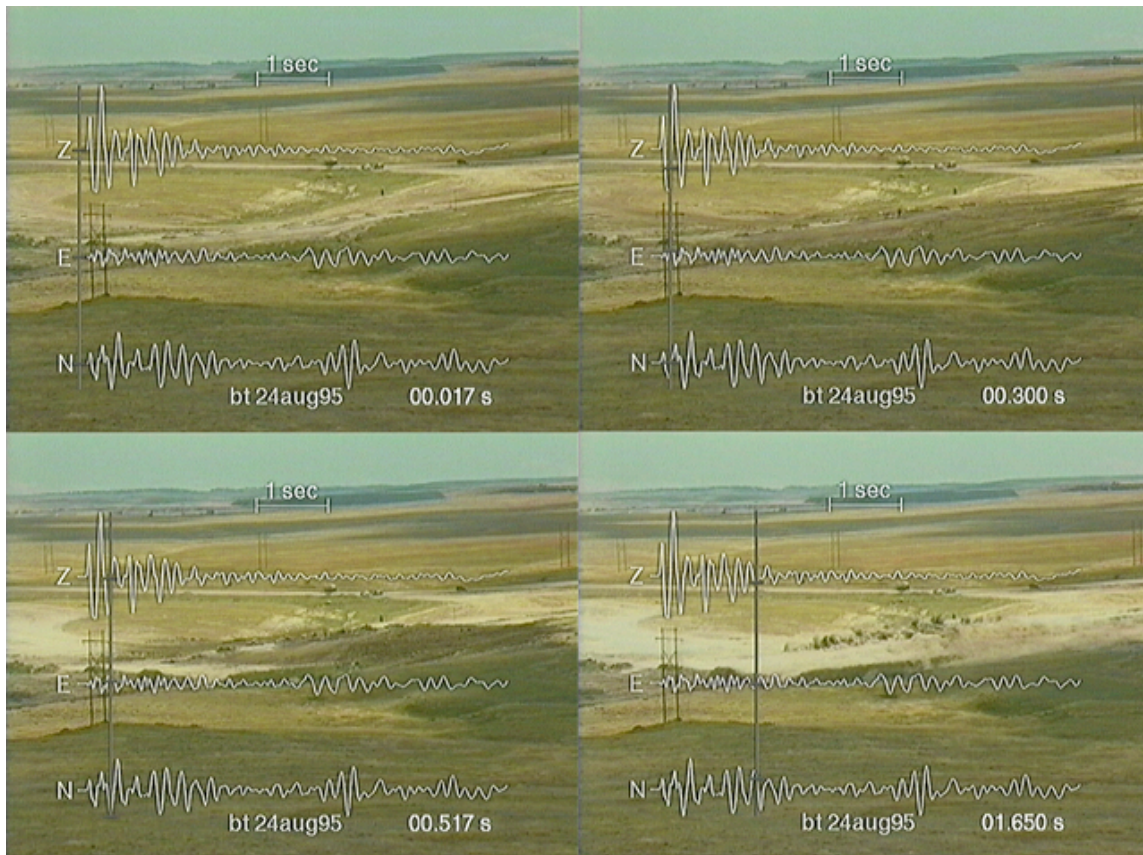


Figure 11a: Video images and time correlated ground motions from a single-fired explosion. The simple, impulsive nature of the waveforms is characteristic of the fact that all eight boreholes were detonated simultaneously. Spall closure of the near-surface layers can be seen in the latter fields as indicated by the ring of dust moving towards the center of the explosive array.

A three-dimensional model of this explosion was created to further investigate the associated physical processes. The topography of the portion of the mine where this explosion was conducted forms the base of the image. The topographic data set was obtained from aerial photography of the mine. As indicated in Figure 11b, it includes the corner of the pit and a portion of the bench behind the pit. The purpose of this initial experiment was to create as simple a source as possible and so the emplacement boreholes were moved from the pit so that there would be no failure of the pit wall. The video images documenting the blast focus on the bench area. The pit in these images (Figure 11a) is just out of view to the lower left.

The detonation time of each individual borehole is represented by the appearance of a small yellow sphere in the model images, which in turn generates a cylindrical red ring that grows in diameter at the appropriate compressional velocity for the media. This model captures some of the three-dimensional aspects of the explosions and subsequent generation and propagation of seismic compressional energy for comparison to the data. Components of the model that replicate the true blast are the spatial and temporal locations of the individual explosions and the



representation of the compressional energy. Many important phenomena are not included such as free surface (or free face) interactions, effects of geological layering and secondary sources such as spall.

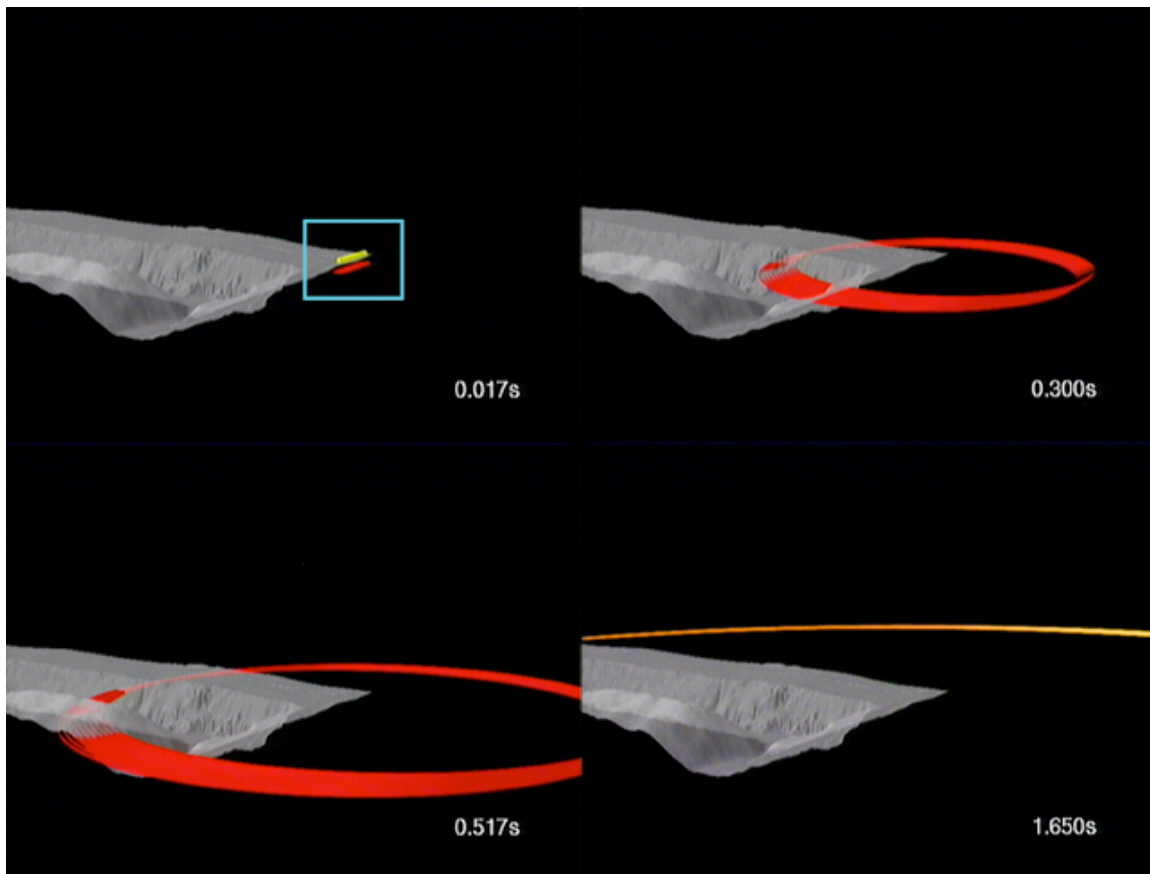


Figure 11b: Model of the single-fired explosion depicted in Figure 11a, the region imaged in the video is outlined in blue in the first picture (0.017s). Ten boreholes at 34-foot spacing are detonated simultaneously, each generating a red ring that expands at the compressional velocity of the material. Even though there are ten individual explosions, the resulting compressional field quickly becomes cylindrical as indicated in the latter frames of the model.

Although the ten boreholes are a line source, the nearly cylindrical nature of the compressional wavefield by the third frame at 0.517 s suggests that a point source assumption is a good one for assessing the waveforms, particularly those at the more distant stations. The model indicates that the initial compressive energy propagates rapidly away from the region imaged in the video sequences. This characteristic is consistent with the earlier interpretation of the near-surface phenomena seen in the 0.517 and 1.650 s images as secondary source process, possibly spall closure.

- **Cast Blast**

Cast blasting for the purpose of overburden removal in coal recovery utilizes delay-fired explosions. This type of explosion is the second blasting example. The explosion consists of an eight row shot with a total of 704 boreholes and 4,738,230 pounds of explosives. The individual boreholes are between 108 and 180 feet

deep with explosive loads from 3,200 to 11,000 pounds. The burden and spacing are 33 and 34 feet respectively. Uphole delays of 35 ms are used between holes in the front row with downhole delays of 125, 300, 500, 700, 900, 1000, 1200 and 1400 ms in an echelon pattern from the front row. This timing pattern and the large spatial dimensions of the shot lead to a relatively complex delay pattern with a total time duration of over 4.5 s.

The video data used in this analysis was taken from within the pit with the shot moving towards the camera (Figure 12a). The ability to deploy a video camera in an unmanned mode was utilized. One can see the 60 feet of coal and the average 160 feet of overburden where the explosives are emplaced. The combination of digitized and de-interlaced video, ground motion and two-dimensional model follows the format discussed earlier. The two-dimensional shot model consists of 704 rectangles that change from white to red at the design shot time, correlated with the appropriate time in the video image. The vertical (Z), transverse (T) and radial (R) ground velocities from a station at approximately 12 km are also time correlated (propagation time for compressional energy subtracted from the waveforms) with the video. The cursor on the ground motion record links them with the time in the video. The ground motion in three-space from the explosion is imaged in the lower right hand corner of the video. This particle motion is diagrammed for a time window whose length is represented by the width of the blue bar following the ground motion cursor.

The first three data images in this example (0.0, 1.25, 4.533 s) document the time duration of the individual explosions while the last one (7.025 s) illustrates that the source duration includes material cast into the pit. There is a 60 image per second movie of this shot including the ground motion and model. The extended duration of the source and resulting ground motions led to introduction of scrolling of the observed waveforms over the image in order to correlate late time ground motions and video images. In the first three images in Figure 12a, the ground motions are stationary and the cursor moves over the ground motion but for the latter times (fourth image) the cursor remains fixed and the early time ground motions scroll off the screen while additional motions appear. This representation illustrates that the source duration, which includes the material cast into the pit, can exceed the total time duration of the shot array.

Correlation of the ground motions with the models illustrates the effect of the number of boreholes detonated per time interval on the amplitude of the ground velocity. Early time ground motions (0.0 to 1.25 s) are small because the explosions in the front row dominate with the 35 ms delay between holes. As the cast blast progresses in time, sources in the back row of the shot begin to detonate as well as those from the front rows. The image at 1.250 s illustrates that shots from the free face to the back row are now involved in the pattern and that the ground motions are building in amplitude. Peak amplitudes are sustained for several seconds and then taper as all the explosions in the front rows are detonated and the pattern is completed in the back rows (4.533 s image). The ground motion continues past this point and as the video image at 7.025 s indicates there is still significant material being cast into the pit. The ground motions at this latter time are distinctly different from those developed during the explosions in that the frequency content is reduced. There are two explanations for this decrease. The first is that the material cast into the pit may be less impulsive as a source. The second is that the ground motion is a result of shear and surface waves as well as compressional energy. The

particle motion diagrams indicate more horizontal motion at latter times supportive of the shear/surface wave interpretation.

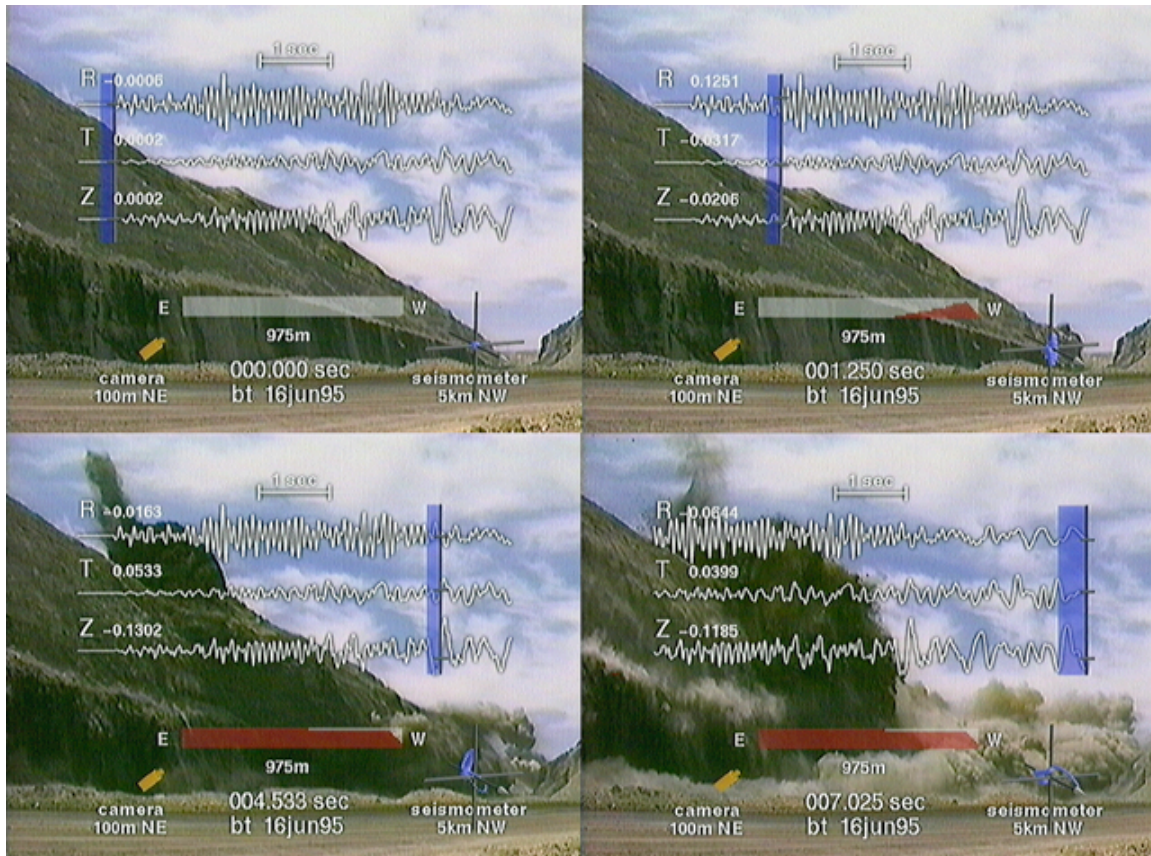


Figure 12a: Video, ground motion and simple two-dimensional model of an open pit cast blast. The source duration is approximately 4.5 s and consists of hundreds of individual detonations.

The movie of this explosion captures subtle differences between individual frames that are not easy to identify in the single images. By playing the movie forward and backwards at different frame rates, one is able to see the interaction of the compressive stress wave from early explosions with the free face of the pit out in front of the detonation process. The stress waves from explosions early in the detonation sequence propagate faster than the delay times between boreholes thus subjecting undetonated boreholes to compressive stress prior to their detonation time.

The three-dimensional model of the cast blast utilizes a three-dimensional image of the pit where the shot was conducted as a base (Figure 12b). The spatial locations of the 704 explosive boreholes are included. As in the previous model, a yellow sphere is imaged at each borehole at detonation time and in turn generates a ring that expands at the compressional velocity of the material. Decay of the compressional energy is modeled with a transition in the color of the ring from red to yellow. The view of the blast is from above the pit with the explosions moving towards the viewpoint. In order to capture the expanding compressional waves, the viewpoint is allowed to move farther from the shot with time.



The first result that can be drawn from the model is the identification of the complex interaction of the seismic waves as a result of the temporal and spatial characteristics of the blast. The source appears as a nearly continuous radiator of seismic energy with the character of individual or groups of individual boreholes lost in the image. The model at 1.25 s is particularly good at representing the complexity in the radiated seismic energy. Three boreholes in different rows are detonating at this time. The compressional energy from previous boreholes has propagated past a number of boreholes that still await detonation. There are complex azimuthal effects in the amplitudes that can be seen by studying the density of wavelets in the images. The 4.53 s image shows these effects quite well. One might expect strong azimuthal variations in the peak amplitudes as a result of these source effects. The number of simultaneously detonating boreholes affects the peak amplitudes as was illustrated with the observational data. This same effect is included in the model and is best illustrated with the end of the shot. The density of wavelets in the tail of the wavefield decreases as a result of the decrease in the number of boreholes detonating in a given time period.

- **Coal Fragmentation**

The third example is an explosion detonated in coal for the purpose of fragmentation. This source was used previously to illustrate the steps in processing the video and other data sets (Figures 5-10). These explosions cast no material and are generally much smaller in total explosive yield and time duration. The shot used in this example consisted of 57 boreholes drilled into the coal to depths of 62 or 63 feet and loaded with 300 to 1600 pounds of explosives each. The total weight of explosives was 77,000 pounds.

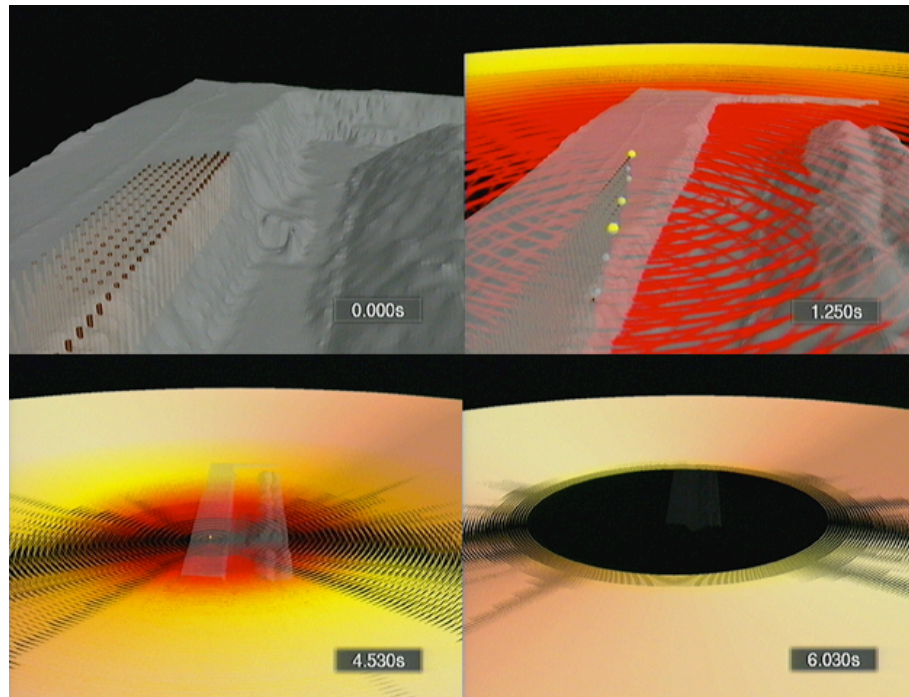


Figure 12b: The model of the cast blast documented in Figure 12a. As in the other models, each individual borehole generates a red ring that expands at the material compressional velocity. The ring color fades to yellow with time. The complex nature of the timing pattern for these explosions results in nearly continuous compressional energy generation.

The video angle for this data set was from the front of the explosion as illustrated in Figure 13a. The right hand side of the shot consists a series of echelon rows that detonate every 42 ms. The left hand side of the shot begins at 93 ms ( $2 \times 42 \text{ ms} + 9 \text{ ms}$ ) and consists of a V of explosives detonating every 42 ms moving away from the camera. The seismic instrument is again approximately 12 km from the shot, 45 degrees west of north.

Comparison of the two-dimensional model with the video and the seismic data illustrates that the duration of the compressional energy (again primarily on the vertical component) is controlled by the temporal duration of the source. The image at 1.267 s documents the completion of the detonations and the resulting decrease in peak ground motion. Latter time, longer period motions in the time series are shear and surface waves generated by these sources.

The camera angle in this case has imaged the surface and front face of the coal. A small amount of venting is observed in a couple of the explosive holes. The material is bulked but nothing of significance is cast or broken away from the coal.



Figure 13a: Video images combined with ground motion and two-dimensional model for a small coal fragmentation shot. These are the images used to demonstrate data processing and model combination in Figures 5-10. The short duration of this type of explosion is quite apparent in the seismic waves.

The model for this explosion is replicated in Figure 13b. No three-dimensional topography was available for this shot and so a simple model consisting of the

individual boreholes was employed, focusing strictly on the temporal and spatial effects of the explosions. The radiated seismic energy from this configuration is far simpler than that observed for the cast shot. The dominance of the 42 ms delay pattern is seen in the evenly spaced groups of seismic waves in the 0.50 and 0.75 s images. Each of these packets of energy is composed of three to six individual rings. The separation of the rings in these packets is a result of both the spatial separations of the individual boreholes as well as the 9 ms delay between the right and left-hand side of the explosive array.

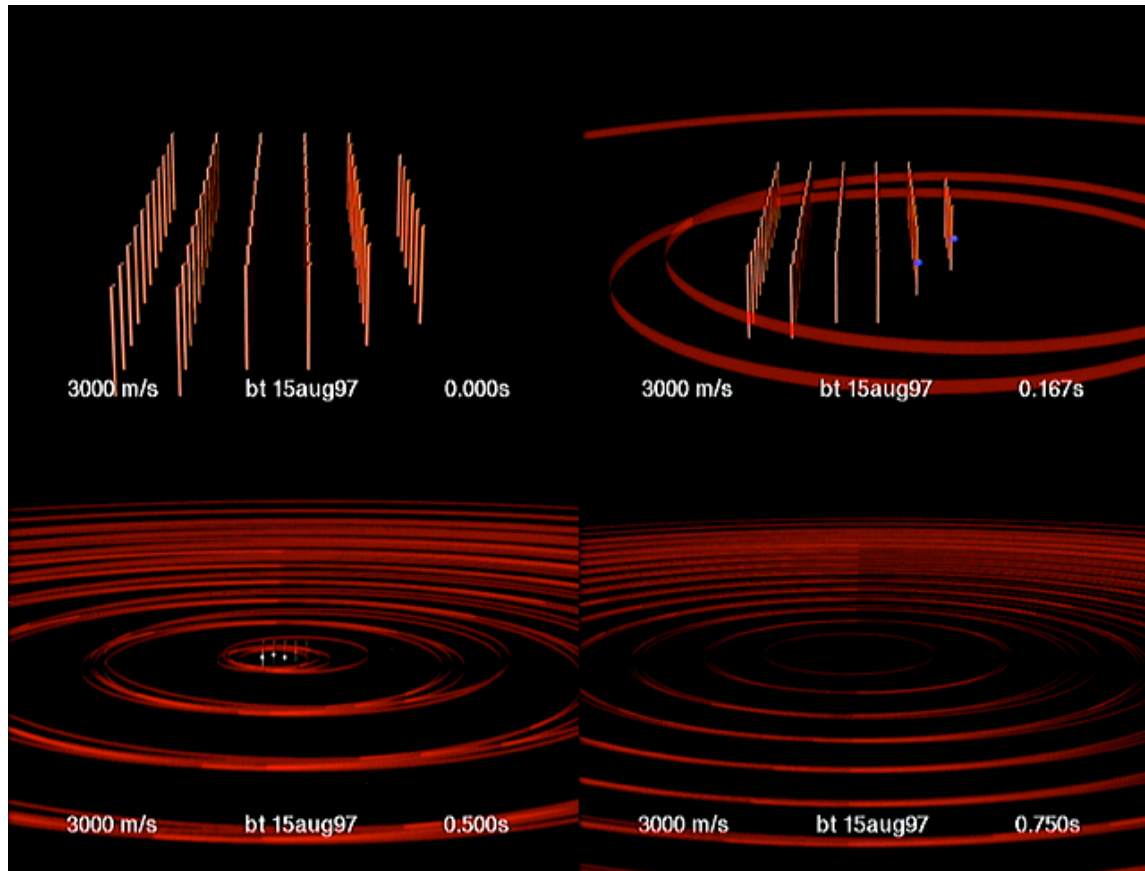


Figure 13b: Three-dimensional model of the coal shot documented in Figure 13a.

- **Hard Rock Fragmentation**

The use of explosives for the purposes of fragmenting hard rock is the fourth example. It is taken from a mine in Southern Russia in the Caucasus that is recovering molybdenum (Stump *et al.*, 1994). The use of explosives in this application is designed to fragment the rock so it can be transported down the mountain for further processing. The mine site is far from any populated area and so the blasting practices are somewhat unconventional. De-interlaced video images are replicated in Figure 14a. One unique aspect of these explosions is that none of the holes are stemmed as documented by the large fireballs emanating from the blast holes at detonation time. Large boulders are often left behind from previous blasting operations and bags of explosives were draped over the boulders with little or no cover. The result is more explosives venting to the atmosphere. These sources are strong sources of acoustic energy.





Figure 14a: Video images from a hard rock fragmentation shot. In this shot each row is detonated simultaneously with a 100 ms delay between rows. Note the lack of stemming and the surface explosions that are captured in the video.

The shot array consisted of six rows of boreholes in addition to the random surface explosives. The shot is modeled in Figure 14b with the individual boreholes represented as dark blue balls superimposed on the actual test site topography. The bags of surface explosives are modeled as orange surface balls. All shot holes in each row of explosives are detonated simultaneously with 100 ms delay between rows. When a borehole detonates, it turns red and generates a blue ring representative of the seismic waves which expands at the material compressional velocity and an orange ring representative of the acoustic energy (surface bags also generate acoustic energy) that expand at the speed of sound in the air. The simultaneous detonation of each row of explosives produces a banded character to the seismic energy much like that observed in the model of the coal shot shown earlier. The simultaneous detonation of each hole in a row is validated by careful inspection of the movie from the de-interlaced video images. The second and third images in Figure 14a illustrate the nearly similar appearance of all boreholes in each row supporting this interpretation.

The model illustrates differences in the propagation characteristics of the seismic energy through the solid earth (blue expanding rings) and the acoustic energy (orange rings) through the atmosphere. The acoustic energy is slower as illustrated in the last image where the last of the seismic energy has cleared the test bed while the acoustic energy is still near the boreholes. The interaction of the acoustic energy



with surface topography is documented in the third image of the de-interlaced video where a condensation ring can be seen around the free face edge. The model (third frame) suggests that the acoustic energy from the initial detonations is just reaching this interface.

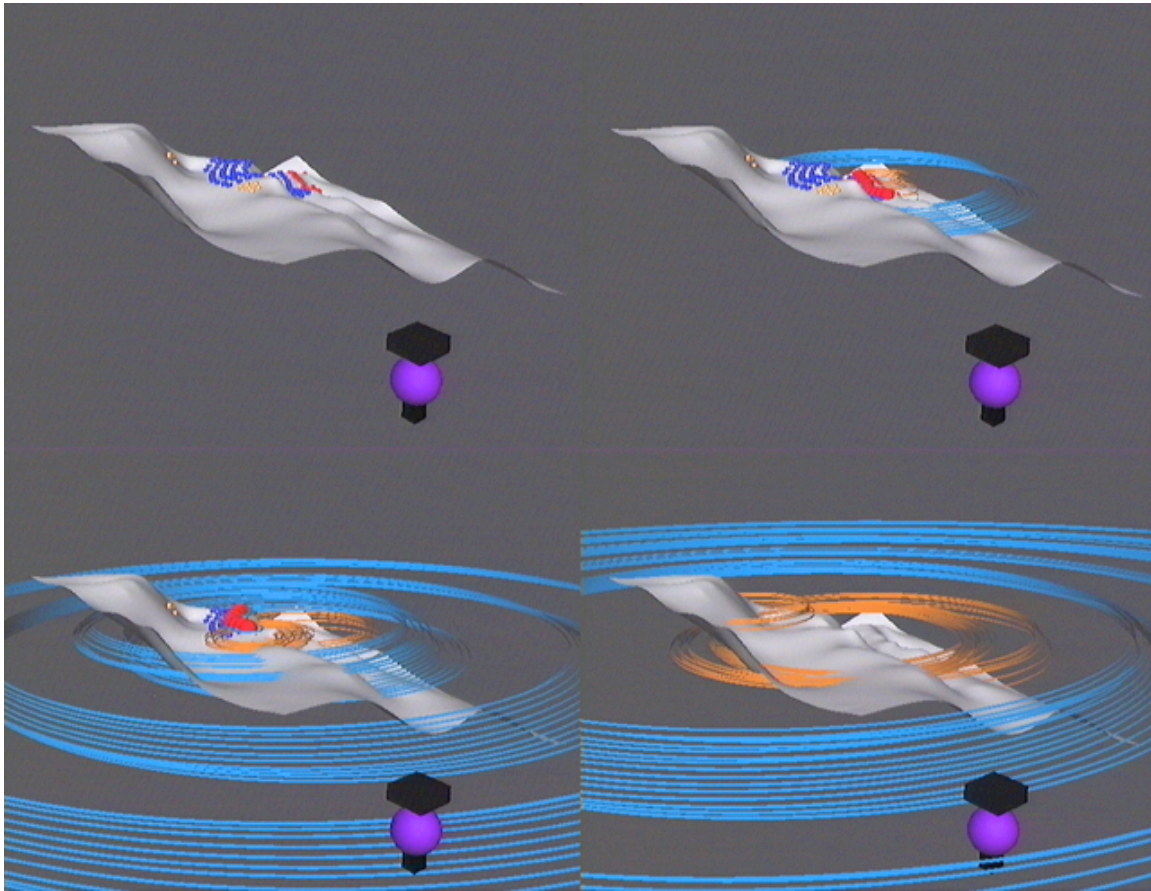


Figure 14b: Model of the rock fragmentation explosion documented in Figure 14a. The individual boreholes turn red at detonation time and generate a compressional wave (blue rings). Since there was no stemming in the holes, acoustic energy was modeled as an expanding orange ring.

- **Soft Rock Bulking**

The final example is the documentation of an overburden explosion designed to bulk material (Figure 15a). The shot consisted of a four-by-four array of 12.4-inch boreholes, each 35 ft deep and loaded with 500 pounds of explosives. Burden and spacing was 30 and 35 feet. The design detonation sequence consisted of 17 ms across the front row with subsequent rows wired to the first, each with 42 ms delays. A low powder factor provided for increased confinement and bulking rather than casting of material. Ground velocities were recorded at a range of approximately 2 km. Absolute time was used to correlate the video and ground motion. The video image of the detonation occurs prior to the seismic records because of the propagation time from the explosion to the receiver. Four images correlated with the seismic data in this manner are reproduced in Figure 15a.

Determination of the importance of the rejoin of the lofted material in these bulking shots to the observed seismic data was one goal. Comparison of the timing of the lofting and rejoin to the seismic data suggests that the rejoin for these bulking shots have little or no contribution to the near-source seismic data (within the bandwidth of the 1 Hz velocity sensor used in this experiment). One can see in the fourth frame of Figure 15a that material is still lofted yet the seismic signal has decayed to background noise levels.

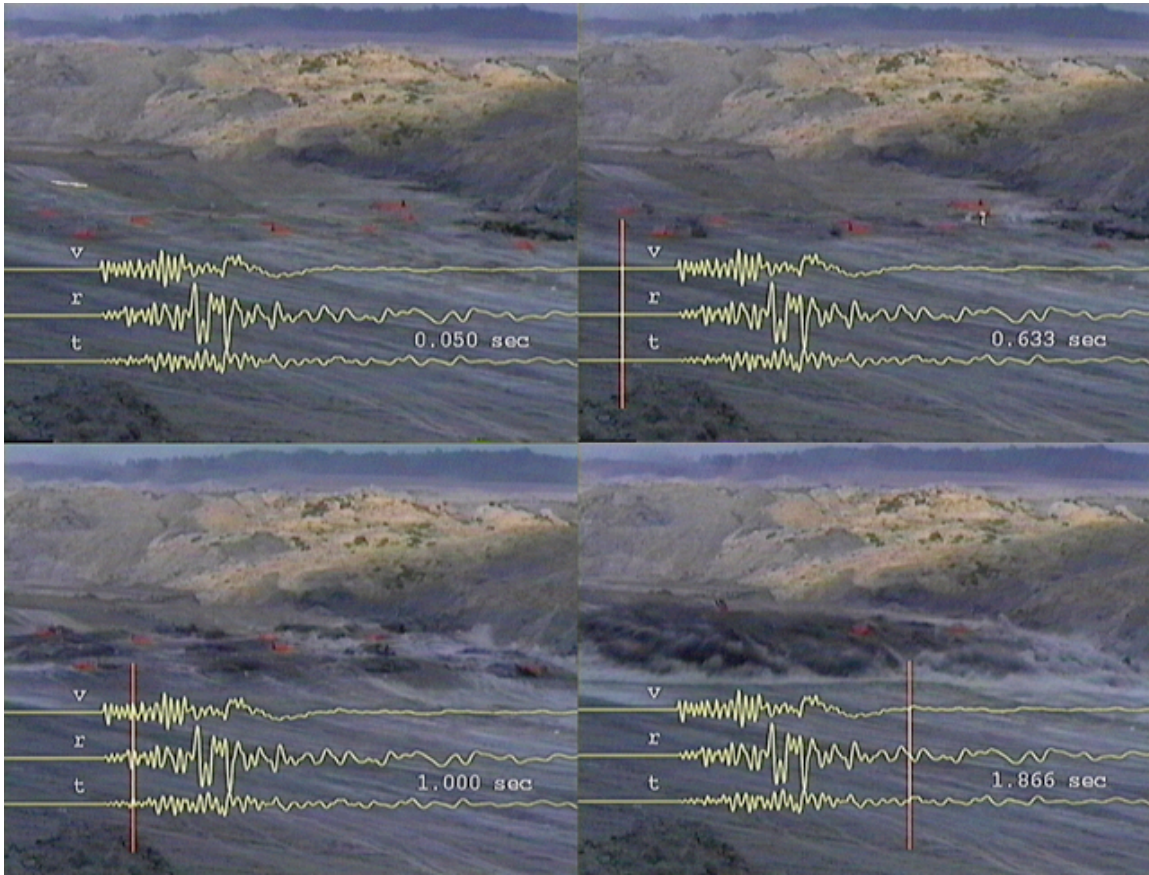


Figure 15a: Soft rock bulking shot. Waveforms and video are aligned in an absolute sense making no correction for propagation time from the explosion to the seismograph.

Documentation of design and actual blasting times was a secondary goal. Velocity of detonation measurements were made in each explosive hole so empirical shot times could be compared to design times. Figure 15b compares the design and actual delay time models to the observational data. There are significant differences between the two since the actual shot pattern departed from the blast design. Between the third and fourth images, three boreholes in the actual sequence detonated very close in time resulting in increased ground motions.

## Analysis of Mining Explosion Performance

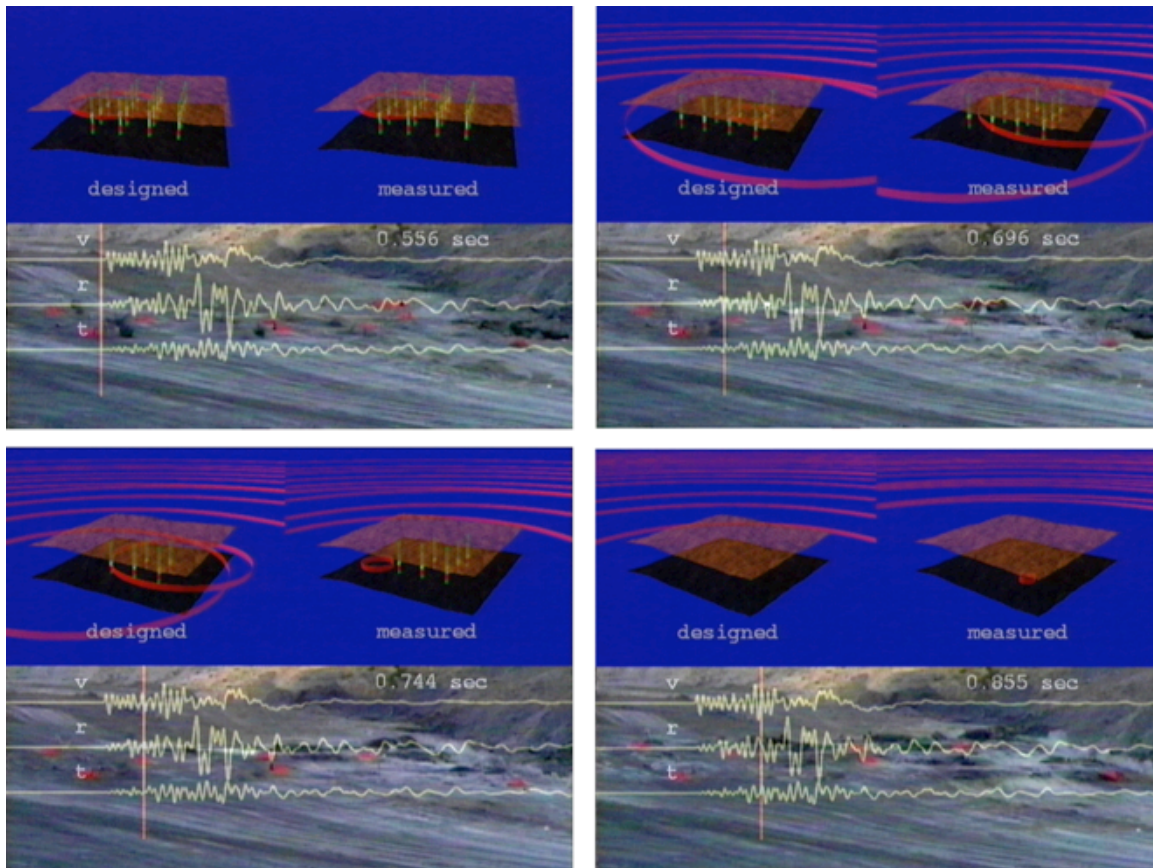


Figure 15b: Comparison of designed and observed delay times to images of the bulking shots.



## **4. Results**

### **• Overcoming Frame Rate Limitations of Video Data**

Video data provides a foundation for interpretation of the other data sets (possibly at a higher sample rate) such as ground motion and acoustic. The higher sample rate of these complementary data sets and models of the blasts can be used to interpolate rapid processes in the explosion that may be under-sampled by the lower frame rate video data.

Video data from the coal shot (60 images/s, 16.67 ms between images) analyzed previously (Figures 5-10, 13) are combined with model data created at 240 images/s (4.16 ms between samples) to illustrate this interpolation procedure. The model was mapped onto the video producing a composite image that can be used for interpretation purposes. Eight images from this composite are reproduced in Figure 16. This eight-image sequence represents one frame or two de-interlaced fields from the original video data. During this time interval, a number of boreholes detonate as represented by the yellow spheres that appear at shot time and generate an expanding ring representative of the compressional energy. One can see a single borehole detonate to the right at 0.523 s and three boreholes simultaneously 8 ms latter.

Although typical video sampling rates are not high enough to capture all blast phenomena, particularly with ms delay firing, the combination of the video with models offers an important interpretational tool for monitoring blasts. Figure 16 illustrates how the effects of closely spaced explosions can then be interpreted in terms of the video and in other examples the resulting seismic data.

### **• Effect of Blast Design on Near-Source Seismograms**

The style of blasting (fragmentation, bulking, and casting) has a strong imprint on the near-source seismograms. Source duration and confinement are the primary contributors to the near-source ground motion. Mining explosions generate both body and surface waves at close distances with the size of intermediate period surface waves strongly linked to blasting practice. These effects have been quantified by correlating wavefield data with blast images.

Source duration has a dominant effect on the observed near-source seismograms, particularly the compressional arrivals. Comparison of the combined video and ground motion records from the single shot (Figure 11a), the coal shot (Figure 13a) and the cast shot (Figure 12a) illustrate the effects of short, intermediate and long duration sources. The compressional energy from the single shot is impulsive with dominant energy for 0.5 s, the coal shot seismogram has a duration of 1 s and the cast shot nearly 5 s. This effect directly reflects the source duration illustrated by the models in Figures 11-13b where the single shot has ten boreholes detonated simultaneously, the coal shot has 57 boreholes detonated over 0.6 s and the cast duration has 704 boreholes detonated over 4.5 s.

Another effect that can be assessed with this data and the models is the generation of secondary arrivals either as a result of secondary source phenomena or later arriving phases such as surface waves. The single shot seismic data is dominated by the compressional arrivals (Figure 11a) with small secondary arrivals.



Figure 16: Eight video images with superimposed 3D model from the coal shot. The model is sampled at 240 images/s and superimposed on de-interlaced video data. The eight images represent 1 video frame or two de-interlaced fields emphasizing the temporal resolution of the video data relative to blast phenomena.



The cast shot (Figure 12a) contains significant energy arriving after the compressional waves and comparison to the video images at the same time indicates that there is still significant material being cast into the pit. It is not possible with the video and ground motion alone to uniquely isolate the cause of these secondary arrivals between the material being cast into the pit and the direct generation of surface wave energy by the individual explosions. The fact that the single shot explosions did not cast material and had relatively weak secondary arrivals suggests that the material cast into the pit in this case may be important in exciting the secondary arrivals.

Comparison of the seismic and video data from the bulking shot (Figure 15a) indicated that the spalled or bulked material did not contribute to late time arrivals. This observation is consistent with the cast observations since the material thrown into the air in the case of the bulking shot re-impacted back to near its original location (no pit). In the case of a cast shot with the deep pit into which the bulked material is thrown, there is a significant vertical difference in the location of the material before the shot and after, releasing potential energy. It is this potential energy release that might account for the robust secondary arrivals in the cast blast seismograms.

- **Different Types of Cast Blasts**

Timing patterns can significantly affect the characteristics of the radiated seismic energy from a blast. A second example of cast blasting is used to illustrate the vast difference in waveforms from two explosions designed for the same purpose. The two cast blasts are from different mines each with their own site-specific requirements.



Figure 17a: Video, ground motion and simple model for a second cast shot in a different mine. This cast shot utilizes a simple shooting pattern where echelon boreholes in each row are detonated every 100 ms. This pattern produces the regular nature of the resulting seismograms.

The combined video, ground motion and simple two-dimensional model for this second cast blast is given in Figure 17a. This explosive array consists of five rows with 89 explosive boreholes in a row. Five boreholes, one in each row along an echelon, are detonated every 100 ms producing a simple source with a total duration of 8.9 s. The resulting compressional energy is simple and homogeneous in amplitude.

The model of the compressional energy from this shooting pattern is reproduced in Figure 17b. It shows the repeated impulses from the detonations every 100 ms. Contrasting this cast shot with the first one (Figures 12a and b) illustrates the strong effect the timing pattern can have on the radiated seismic energy. The earlier cast blast produced a much more complex pattern of compressional energy with seismic amplitudes building during the detonation process but no repeatable pattern identified.

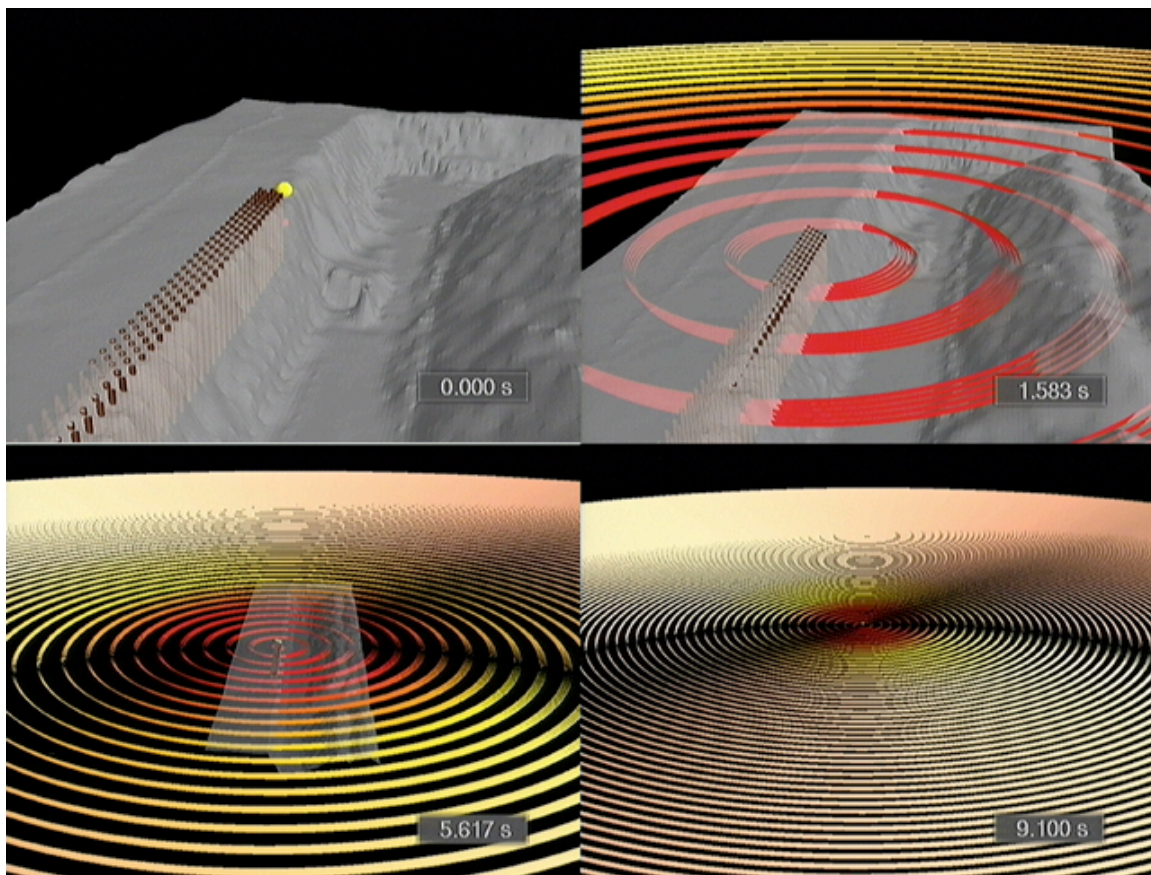


Figure 17b: Model of the coal cast shot documented in Figure 17a. The repetitive nature of the blasting pattern (every 100 ms) leads to the regular banding in the seismic waves.

- **Multiple Angle Images of Blast**

Three-dimensional models of large engineering explosions such as those associated with cast blasting illustrate the complexity and spatial extent of these sources (Figure 12b and 17b). These characteristics support a need for multiple cameras to completely document the explosion. As illustrated in Figure 12b some of these deployments such as those in the pit must be unmanned. Standard,



modest cost video cameras that are time synchronized provide the means for such documentation. An illustration of such a deployment on a large cast shot is made.

The shot consisted of 984 holes in eight rows with a total charge weight of 8,328,398 pounds. Uphole delays of 35 ms were used in the front row of the shot. Two downhole delays were used in each borehole, a shorter one at the toe and a slightly longer one at the top. Moving from the front row to the back, the downhole delay pairs were 200/250, 400/450, 600/650, 800/850, 1000/1100, 1200/1300, 1400/1500 and 1600/1700 ms. Shot design was similar to but larger than the cast shot documented in Figure 12a and modeled in Figure 12b. The first camera location was on the spoils pile overlooking the west end of the shot with the detonation sequence moving away from the camera (Figure 18a). The shot appears to perform well in this image, although the end of the shot away from the camera is not well imaged. The waveform data that is superimposed on the video documents a large amplitude event at 4.3 s. It is hard to identify anything in the video from this camera angle to correlate with this signal.

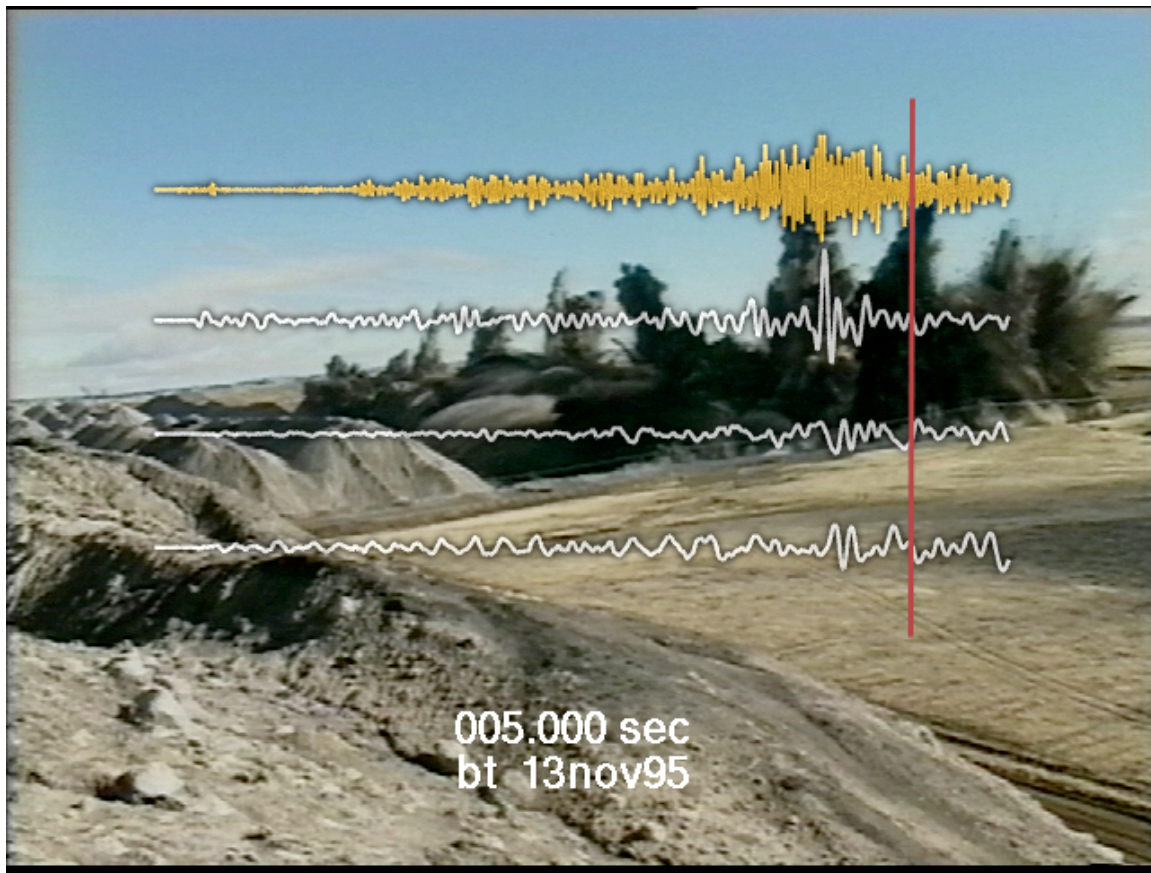


Figure 18a: Video, acoustic (yellow) and ground motion (white – vertical, north/south, and east/west) waveforms of the cast blast. The video is taken from the west end of the shot with the detonation sequence moving away from the observer.

The second camera in this experiment was in the pit at the east end of the shot with the detonation sequence moving towards it. This installation provided a good record of phenomena in the pit at the end of the shot. The combined video, ground motion, acoustic and model images are reproduced in Figure 18b. The early parts

of the explosion perform as designed with a smoothly progressing detonation front and the gradual increase in amplitude of the seismic records as the overlap of detonations in the front and back rows of the charge array increase.

This camera angle provides data for interpreting the large amplitude seismic energy that occurs at 4.3 s. Careful examination of the combined video, ground motion, acoustic, and model data in movie format suggests that the simultaneous detonation of a large number of boreholes at the end of the shot may be responsible for the large amplitude seismic arrival. The end of the explosive array did not follow the design timing sequence but instead detonates simultaneously, producing a large acoustic and seismic signal as well as blowing out the entire end of the shot. Some of the resulting material that was cast eventually engulfed the documentation camera illustrating why such instruments must be unmanned and not prohibitively costly.

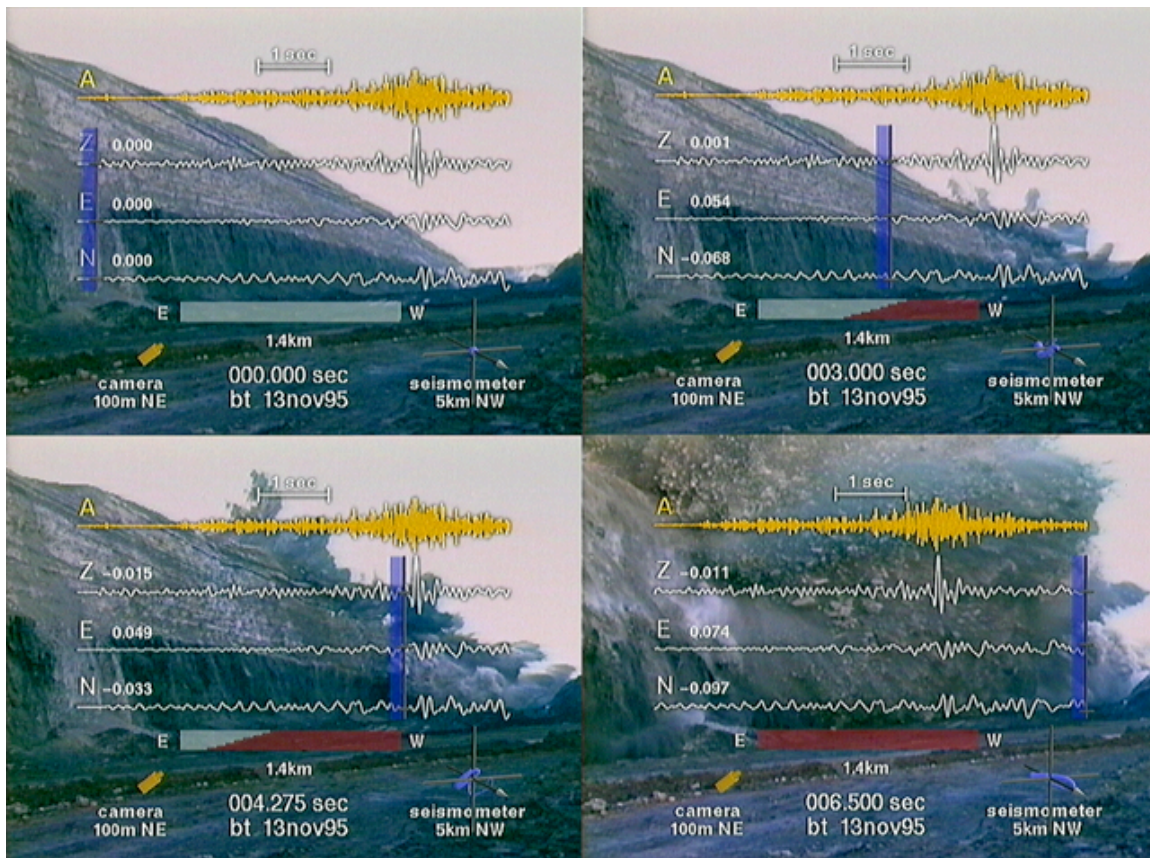


Figure 18b: Video, ground motion (white), acoustic (yellow) and simple model of a cast blast. This shot included the anomalous, simultaneous detonation of many boreholes at approximately 4.3 sec (third image) that is the cause of the large vertical spike in the ground motion.

A three-dimensional blast model illustrates what occurred during the detonation (Figure 18c). The shot begins in normal fashion moving down the free face with 35 ms between detonations in the first row and then the subsequent detonations of the back rows as a result of the downhole delays. It is this initial part of the shot that the camera on the west end captured. At the east end of the shot, the data suggests that many boreholes detonated in a very rapid time period out of sequence producing the observed impulsive seismic signal.



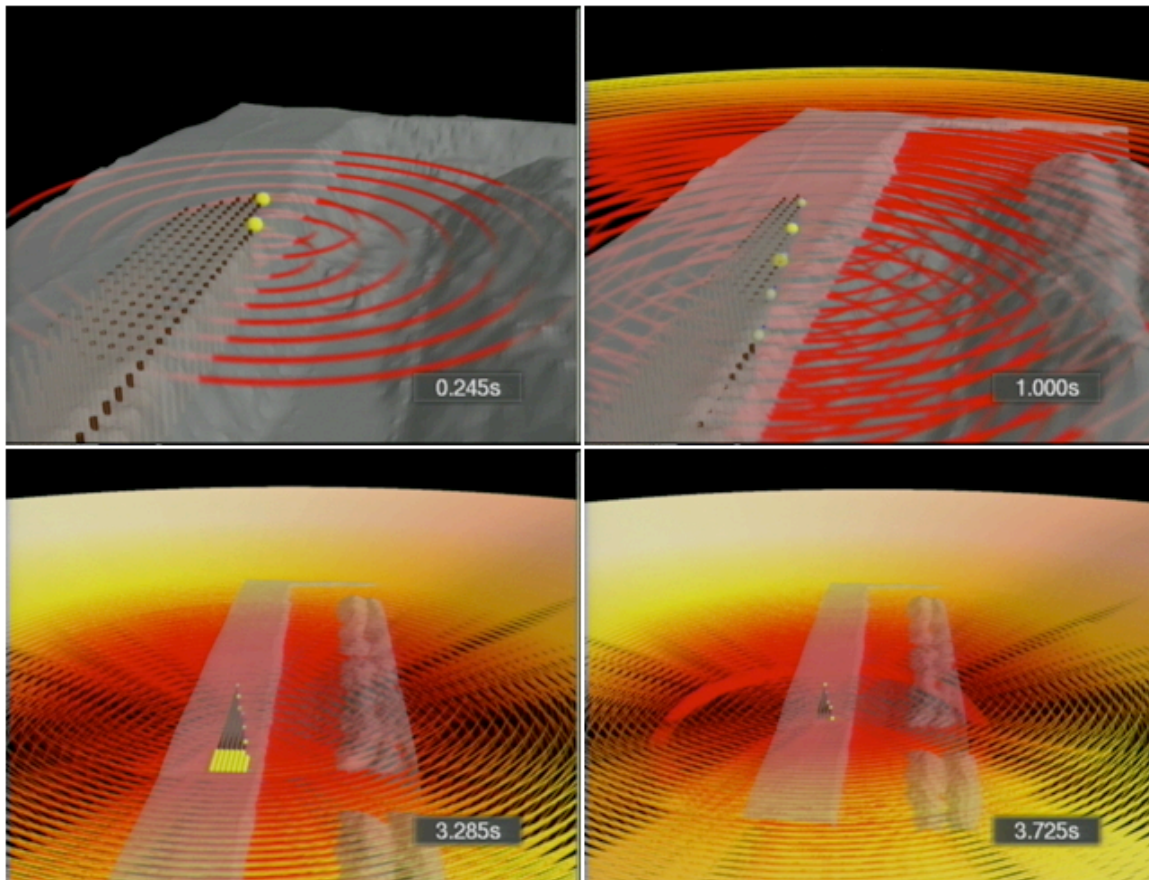


Figure 18c: Model of the interpreted detonation sequence for an anomalous cast blast .

- **Documentation of Damage**

Video data can be used to quantify the effects of the mining explosion on the rock around each of the explosive boreholes. An overburden-casting explosion designed to expose a coal seam is used to illustrate this application (Figure 19). As the images in this example demonstrate, the explosions are not only moving the overburden but they are damaging the coal as well. The coal damage was attributed to a problem in depth control of the individual boreholes used for explosive emplacement. The video data processed in a timely manner provided the necessary information to solve such problems and reduce the amount of coal damage in future shots. The spatial resolution and dynamic range rather than the sample rate of the video data is the limiting factor.





Figure 19: Four video images from a shallow overburden cast blast. Evidence for damage to the coal during the blast is seen in the image at 1.017 s and 4.333s.

## **5. Conclusions**

The key to the tools and techniques introduced in this paper is the utilization of multiple data sets and models of blasts in digital format. With the rapid development of desktop computing resources, the ability to process a variety of different data sets in digital form from mining explosions and display them together for rapid interpretational purposes will provide new tools for the mining engineer. Examples from a variety of mining explosions have been presented that combine digital image data with ground motion and acoustic data. Relatively simple two and three-dimensional models of the explosions are also used with these observations to help interpret important physical processes accompanying the explosions.

The new tools were designed to utilize existing capabilities and equipment common in many mines, to minimize costs, and to be relatively simple to implement. Video data after de-interlacing provides 60 fields/s and with interpolation 120 images/s. The images are the fundamental data set to which other types of data are added. Visual sample rates are not high enough for characterizing some blast phenomena but have been found quite useful for most applications. The lower sample rate data have been extended when combined with more easily accessible higher sample rate seismic and acoustic data. The image data can be further supplemented with high sample rate models of the blast, which aid in the interpolation of phenomena that occur more rapidly than the image data.

Video cameras exist in almost every mine and are a tool, which is readily available to the blaster. They can be deployed to multiple sites around a single explosion and left in an unmanned mode providing increased safety. It is especially useful to interact with the combined images of the blasts at a variety of speeds ranging from the study of still images (included in this paper) to movies at different speeds (included in accompanying CD). The incorporation of models in this data analysis has provided the opportunity to identify departures from the explosion design.

Multiple cameras have been found necessary to quantify large explosions. Data from the different cameras are best linked through the inclusion of an absolute time base such as GPS for all data acquisition. The anomalous cast blast with the large sympathetic detonation at the end of the shot (Figure 18) best illustrates the usefulness of multiple cameras. An unusually large peak ground motion was not easily interpreted when these records were correlated with video images overlooking the entire shot (Figure 18a). It was only when video data from a second camera in the pit was included in the analysis that the sympathetic detonation was identified (Figure 18b). This second camera was in an area inaccessible by humans at shot time and illustrates the attribute of robust recording systems that can be left unattended for time periods approaching one hour.

Two and three-dimensional models of the blasts and some of the accompanying physical phenomena such as seismic and acoustic wave propagation have been incorporated into the analysis. These models provide the opportunity to refine the interpretation of temporal and spatial effects observed in the data. The regular delay patterns of some of the mining explosions are shown to produce impulsive seismic waves while other complicated delay patterns such as those associated with some types of cast blasts are shown to be more continuous radiators of energy. The two-dimensional blast models were found to be useful for interpreting timing effects while the three-dimensional models were more helpful in resolving spatial effects. Since the video data is in digital form, it is possible to map the three-dimensional blast

models directly onto the video data in the proper perspective further enhancing the analysis. The models can be produced at higher temporal resolution than the video images and were used to help interpolate between individual video images and identify phenomena that might not be sampled.

The blasting application has significant impact on the character of the seismic and acoustic data recorded in the mine. Source duration was found to be a dominant effect on the observed compressional energy. Simple blasting patterns are found to result in banding of seismic energy resulting in predictable constructive and destructive interference in the radiated wave field. Some types of multi-row cast blasts because of the complex delays result in a more continuous radiation of compressive seismic energy. Secondary sources such as material lofted or spalled is not found to contribute in a significant way to the observed wavefield unless the material is thrown into a pit such as in a casting application. The free fall of material into the pit releases potential energy that may be responsible for late-time, long-period arrivals in the observed ground motions.

Design and actual blasting patterns are found to diverge. The combination of video, ground motion and models has provided documentation of out of sequence blasts as well as relative large sympathetic detonations. The out of sequence detonations can affect the productivity of the shot. The sympathetic detonations were found to produce anomalously large near-source amplitudes as well as problematic casting. The documentation provides the opportunity for correcting these effects.

Finally, the digital video documentation and the ability to look at the blast an image at a time provides the mechanism for assessing damage. Such documentation used iterative in conjunction with the drilling program may provide a mechanism for minimizing unwanted effects such as coal damage.



## **6. Future Development of New Tools**

This research has suggested avenues needing further development. The tools introduced will be most useful to the blasting engineer if they can be applied in near real-time including the synergy of the different data sets. Such an application will provide quick feedback on blasting for subsequent application and improvement. The analysis tools have been developed with this need in mind. A completely integrated PC based system is suggested to meet this requirement.

Critical to the combination of the different data sets is their correlation in space and time. It is important to record the spatial locations of instruments during these experiments as well as acquire three-dimensional topographic data sets. Correlation in time for the most part was completed through visual inspection of the different data sets. Global Positioning System (GPS) receivers provide the opportunity for accurate and precise spatial and temporal determinations. Many mines are already using such systems for surveying and equipment tracking. A number of commercially available acoustic and seismic data acquisition systems already utilize the technology. Methods exist for writing GPS time and location to the video data as well. An integrated data acquisition system based around GPS would provide the mechanism for linking the different observational data sets in a quantitative manner.

The three-dimensional data sets and models employed in this study are rather crude. It is important to extend these models to more complete subsurface characterization in two and three-dimensional subsurface structure.

The utilization of acoustic data has been minor in this paper illustrating the concept. Full exploitation of this data type for source diagnostics needs further work. Development and inclusion of additional quantitative measures such as free face velocities, fragmentation measures and material cast distances should also be completed.

## **7. References**

Chung, S., 1998. Digital imaging techniques for blasting process evaluation in the field, *Proceedings of the Twelfth Symposium on Explosives and Blasting Research, International Society of Explosive Engineers*, 4-8 February, 1996, Orlando, Florida.

Pood, E. and R. Gilbert, 1996. The use of inexpensive video technology for shot analysis and blasting training in the commercial explosive industry, *Proceedings of the Twelfth Symposium on Explosives and Blasting Research, International Society of Explosive Engineers*, 4-8 February, 1996, Orlando, Florida.

Reamer, S. K., K.-G. Hinzen and B. W. Stump, 1992. Near-source characterization of the seismic wavefield radiated from quarry blasts, *Geophys. J. Int.* 110, 435-450.

Stump, B. W., D. P. Anderson and D. Craig Pearson, 1996. Physical Constraints on Mining Explosions: Synergy of Seismic and Video Data with Three Dimensional Models, *Seism. Res. Letters*, 67, 9-24.

## **8. Acknowledgments**

This paper has involved critical contributions from many individuals. The personnel at the Black Thunder Coal Mine - Dave Gross, Al Blakeman, Terry Walsh, and the Bridger Coal Mine - Chris Frandsen, provided exceptional support in the mines and insight into modern blasting practices. Portable instruments were deployed by Los Alamos National Laboratory - C L Edwards, Diane Baker, and Roy Boyd. The field crew provided excellent data and sparked important discussions that led to the resulting analysis. Work on this paper for two of the authors (BWS and DCP) was performed under the auspices of the US Department of Energy by Los Alamos National Laboratory under contract W-7405-ENG-36. David P. Anderson under US Department of Energy and Los Alamos National Laboratory contract 6341N0015-3P developed visualization and imaging tools.